J|A|C|S
ARTICLES
Published on Web 08/27/2005

Extraordinary Cluster Formation and Intramolecular Ligand−Ligand Interactions in Cyanoactylene Mediated by $Mg^{+\bullet}$: Implications for the Atmospheric Chemistry of Titan and for Circumstellar Chemistry

Rebecca K. Milburn, Alan C. Hopkinson,* and Diethard K. Bohme*

Contribution from the Department of Chemistry, Centre for Research in Mass Spectrometry and Centre for Research in Earth and Space Science, York University, Toronto, Ontario, Canada M3J 1P3

Received May 20, 2005; E-mail: dkbohme@yorku.ca

Abstract: Experimental results are reported that track the kinetics of gas-phase reactions initiated by $Mg^{+\bullet}$, $(c\text{-}C_5H_5)Mg^+$ and $(c\text{-}C_5H_5)_2Mg^{+\bullet}$ in hydrogen cyanide and cyanoacetylene. The experiments were performed with a selected-ion flow tube (SIFT) tandem mass spectrometer at a helium buffer-gas pressure of 0.35 ± 0.01 Torr and at 294 ± 3 K. The observed chemistries of $Mg^{+\bullet}$ and $(c\text{-}C_5H_5)Mg^+$ are dominated by sequential ligation, while that of $(c\text{-}C_5H_5)_2Mg^{+\bullet}$ is by ligand switching. The rate-coefficient measurements for sequential addition of cyanoacetylene to $Mg^{+\bullet}$ indicate an extraordinary pattern in alternating chemical reactivity while multiple-collision induced dissociation experiments revealed an extraordinary stability for the $Mg(HC_3N)_4^{+\bullet}$ cluster ion. Molecular orbital calculations with density functional theory (DFT) at the B3LYP level, Hartree−Fock (HF) and second-order Mϕller−Plesset (MP2) levels, all performed with a 6-31+G(d) basis set, have been used to calculate structures and energies for the observed $Mg(HC_3N)_{1-4}^{+\bullet}$ cations. These calculations indicate that the path of formation of $Mg(HC_3N)_4^{+\bullet}$ involves ligand−ligand interactions leading to two cyclic $(HC_3N)_2$ ligands which then interact to form 2,4,6,8-tetracyanosemibullvalene-Mg^+ or 1,2,5,6-tetracyano-1,3,5,7-cyclooctatetraene-Mg^+ cations**.** A case is made for the formation of similar complex organomagnesium ions in the upper atmosphere of Titan where subsequent electron−ion recombination may produce cyano derivatives of large unsaturated hydrocarbons. In contrast, circumstellar environments with their much higher relative content of free electrons are less likely to give rise to such chemistry.

1. Introduction

Ongoing interest in gas-phase atomic magnesium and organomagnesium ion chemistry has prompted us to extend our earlier studies of reactions of $Mg^{+\bullet}$, $(c\text{-}C_5H_5)Mg^+$, and $(c\text{-}C_5H_5)_2Mg^{+\bullet}$ with inorganic molecules[1,2] and saturated hydrocarbons[3] to hydrogen cyanide and cyanoacetylene. We have chosen these latter reactants mainly for the importance of these molecules in several planetary and circumstellar environments, both of which can contain magnesium. For example, the Voyager mission to Saturn has revealed that cyanoacetylene is the third most abundant nitrogen compound in Titan's atmosphere, after N_2 and HCN.[4] Atomic magnesium ions are produced in this atmosphere by thermal ablation of cosmic dust particles,[5] as is the case in the planetary atmospheres of Earth, Mars, and Jupiter.[6] Hydrogen cyanide and cyanoacetylene, and many other related cyanides and isocyanides, are known interstellar/circumstellar molecules that have been identified by radioastronomers.[9] There also have been reports of the detection of the cyanide[7] and isocyanide[8] of magnesium, MgCN, and MgNC respectively, toward the late-type star, IRC +10261, where these molecules are believed to be formed in the outer circumstellar envelope in which the temperature and pressure are sufficiently low for ion−molecule reactions to occur.

Kawaguchi et al.[10] have suggested that MgNC in IRC +10216 is formed by the radiative association reaction 1, followed by dissociative recombination with electrons according to reaction 2, and an analogous reaction sequence has been suggested for

$$Mg^{+\bullet} + HCN \rightarrow MgNCH^{+\bullet} + h\nu \tag{1}$$

$$MgNCH^{+\bullet} + e \rightarrow MgNC + H^{\bullet} \tag{2}$$

the formation of MgCN from CNH.[7] There has been no previous report of laboratory measurements of the reaction of Mg^+ with

(1) Milburn, R. K.; Baranov, V. I.; Hopkinson, A. C.; Bohme, D. K. *J. Phys. Chem. A* **1998**, *102*, 9803.
(2) Milburn, R. K.; Baranov, V. I.; Hopkinson, A. C.; Bohme, D. K. *J. Phys. Chem. A* **1999**, *103*, 6373.
(3) Milburn, R. K.; Frash, M. V.; Hopkinson, A. C.; Bohme, D. K. *J. Phys. Chem. A* **2000**, *104*, 3926.
(4) (a) Francisco, J. S.; Richardson, S. L. *J. Chem. Phys.* **1994**, *101*, 7707. (b) Kunde, V. G.; Aikin, A. C.; Hanel, R. A.; Jennings, D. E.; Maguire, W. C.; Samuelson, R. E. *Nature* **1981**, *292*, 686.
(5) Molina-Cuberos, G. J.; Lammer, H.; Stumptner, W.; Schwingenschuh, K.; Rucker, H. O.; López-Moreno, J. J.; Rodrigo, R.Tokano, T. *Planet. Space Sci.* **2001**, *49*, 143.
(6) Pesnell, W. D.; Grebowsky, J. M. *Adv. Space Res.* **2001**, *27*, 1807.
(7) Ziurys, L. M.; Apponi, A. J.; Guélin, M.; Cernicharo, J. *Astrophys. J.* **1995**, *445*, L47.
(8) Guélin, M.; Lucas, R.; Cernicharo, J. *Astron. Astrophys.* **1993**, *280*, L19.
(9) Herbst, E. *Annu. Rev. Phys. Chem.* **1995**, *46*, 27.
(10) Kawaguchi, K.; Kagi, E.; Hirano, T.; Takano, S.; Saito, S. *Astrophys. J.* **1993**, *406*, L39-L42.

10.1021/ja053302f

either HCN or CNH or for the electron recombination of $MgNCH^+$ and $MgCNH^+$. Computations using variational transition-state theory have predicted a rate coefficient for reaction 1 of 1.0×10^{-16} cm^3 molecule^{-1} s^{-1} at 100 K and a slightly larger rate coefficient of 1.9×10^{-16} cm^3 molecule^{-1} s^{-1} for the analogous reaction with HNC.[11] A theoretical case also has been made for the formation of MgNC from cyanopolyenes as illustrated with cyanoacetylene in the reaction sequence 3 to 4.[12]

$$Mg^{+\bullet} + HC_3N \rightarrow MgNC_3H^{+\bullet} + h\nu \qquad (3)$$

$$MgNC_3H^{+\bullet} + e \rightarrow MgNC + C_2H^{\bullet} \qquad (4)$$

There are no previous reports of the laboratory measurement of the rate coefficient of the radiative association reaction 3, but it has been calculated to be 7.00×10^{-14} cm^3 molecule^{-1} s^{-1} (1.45×10^{-5} times the collision rate) at 300 K and to increase to 2.00×10^{-11} cm^3 molecule^{-1} s^{-1} (7.6×10^{-4} times the collision rate) at 10 K.[12] Reaction 4 also has not been measured in the laboratory, and its products are a matter of conjecture.[12a,c] For example, neutralization to form Mg and to recover HC_3N cannot be excluded.

The chemistry of $Mg^{+\bullet}$ with HCN and HC_3N in the upper atmosphere of Titan very recently has been discussed by Petrie.[13] A case is made for the ligation and multiple ligation of $Mg^{+\bullet}$ with these cyanides by association and ligand-switching reactions that lead to such ligated ions as $MgNCH^{+\bullet}$, HCN-$MgNCH^{+\bullet}$, $MgNC_3H^{+\bullet}$, and $HC_3NMgNCH^{+\bullet}$. A preference was noted for the ligation with HC_3N because of the stronger bonding with this molecule.

In the study reported here, the reactivities of $Mg^{+\bullet}$ with HCN and HC_3N were assessed through measurements of reaction products and reaction rate coefficients at room temperature and at a buffer-gas helium pressures of 0.35 Torr. Under these operating conditions ligation can occur by termolecular reactions of type 5.

$$MgL_n^{+\bullet} + L + He \rightarrow MgL_{n+1}^{+\bullet} + He \qquad (5)$$

Rate coefficients for such ligation reactions are sensitive to the lifetime of the intermediate against dissociation back to reactants that in turn depends on the ligand bond energy, $D(Mg^+{-}L)$, and the size of the ligand (the degrees of freedom in $(MgL^+)^*$ effective in intramolecular energy redisposition in the transient intermediate).[14] This is because the gas-phase ligation proceeds in two steps, reactions 6a and 6b, and the lifetime of the intermediate $(MgL_{n+1}^{+\bullet})^*$ against dissociation back to reactants determines the probability of collisional stabilization in the second step.

$$MgL_n^{+\bullet} + L \leftrightarrow (MgL_{n+1}^{+\bullet})^* \qquad (6a)$$

$$(MgL_{n+1}^{+\bullet})^* + He \rightarrow MgL_{n+1}^{+\bullet} + He \qquad (6b)$$

Also of interest, from the organometallic chemistry point of view, is the influence of ligation on the reactivity of the bare magnesium cation toward cyanides. Because magnesocene was used as the parent gas for the production of $Mg^{+\bullet}$ in the experiments reported here, it was relatively straightforward to also investigate the changes in $Mg^{+\bullet}$ reactivity upon ligation with one and two cyclopentadienyl radicals. We therefore report rate measurements and intercomparisons for both primary- and higher-order reactions of $Mg^{+\bullet}$, $(c\text{-}C_5H_5)Mg^+$, and $(c\text{-}C_5H_5)_2$-$Mg^{+\bullet}$ with HCN and HC_3N. *Multi*-CID experiments were performed with the product ions to provide insight into their bond-connectivities (based on patterns of fragmentation) and into their stabilities (based on measured onsets of dissociation). This combined approach was useful in the elucidation of the remarkable ligand-ligand interactions that are found to be mediated by $Mg^{+\bullet}$.

2. Experimental Section

The experiments were performed using a selected-ion flow tube (SIFT) apparatus that has been described in detail elsewhere.[15] The reactant $Mg^{+\bullet}$, $(c\text{-}C_5H_5)Mg^+$, and $(c\text{-}C_5H_5)_2Mg^{+\bullet}$ ions were produced in a low-pressure (open) ion source by electron-impact ionization of pure magnesocene vapor at electron energies between 35 and 50 eV. The ions produced in the source were mass-selected through a quadrupole mass filter, introduced into the flow tube via a Venturi aspirator, and allowed to thermalize by collisions (about 4×10^5) with helium buffer-gas atoms before entering the reaction region further downstream. The reactant neutrals were added as pure gases, and the variation in reactant and product ion signals was monitored as a function of added reactant neutral with a second quadrupole mass filter at the end of the reaction region. The hydrogen cyanide and cyanoacetylene were prepared with established laboratory procedures and used without further purification.[16]

All measurements were performed at a room temperature of 294 ± 3 K and at a helium operating pressure of 0.35 ± 0.01 Torr. Rate coefficients and product distributions were measured in the usual manner.[15] Apparent bimolecular rate coefficients for primary reactions were obtained from a fit to the pseudo-first-order semilogarithmic decay of the primary ion with added neutral reactant. Rate coefficients for higher-order reactions were obtained by fitting the higher-order ion profiles to the solutions of the appropriate differential equations for sequential reactions. Also, in separate experiments, ligated ions were deliberately subjected to multicollision induced dissociation (CID) just prior to sampling by changing the potential of the sampling nose cone. The operation, advantages, and limitations of this CID technique have been described in detail elsewhere.[17] Because of multicollision conditions, the CID measurements are used primarily to ascertain bond connectivities and to provide insight into *relative* binding energies.

3. Theoretical Section

Standard ab initio molecular orbital calculations were performed using the *Gaussian 98* program.[18] The density functional Becke three-parameter hybrid method[19] that includes the Slater (local spin density) exchange functional with nonlocal gradient-corrected terms[19a,b,20] and the Lee−Yang−Parr method,[21,22] which includes local and nonlocal gradient corrected correlation functional, were used to optimize geometries. Use of this procedure with a basis set of 6-31+G(d) will

(11) (a) Petrie, S.; Dunbar, R. C. *J. Phys. Chem. A* **2000**, *104*, 4480. (b) Petrie, S. *J. Phys. Chem. A* **2003**, *107*, 10441.
(12) (a) Petrie, S. *Mon. Not. R. Astron. Soc.* **1996**, *282*, 807. (b) Dunbar, R. C.; Petrie, S. *Astrophys. J.* **2002**, *564*, 792. (c) Petrie, S. *Mon. Not. Not. R. Astron. Soc.* **1999**, *302*, 482.
(13) Petrie, S. *Icarus* **2004**, *171*, 199.
(14) See, for example: Tonkyn, R.; Roman, M.; Weisshaar, J. C. *J. Phys. Chem.* **1988**, *92*, 92.
(15) (a) Mackay, G. I.; Vlachos, G. D.; Bohme, D. K.; Schiff, H. I. *Int. J. Mass Spectrom. Ion Phys.* **1980**, *36*, 259. (b) Raksit, A. B.; Bohme, D. K. *Int. J. Mass Spectrom. Ion Processes* **1983**, *55*, 69.
(16) (a) Glemer, O. In *Handbook of Preparative Inorganic Chemistry*; Brauer, G., Ed.; Academic Press: New York, 1963; p 658. (b) Moureu, C.; Bongrand, J. C. *Ann. Chim. (Rome)* **1920**, *14*, 47.
(17) Baranov, V. I.; Bohme, D. K. *Int. J. Mass Spectrom. Ion Processes* **1996**, *154*, 71.
(18) Frisch, M. J. et al. *Gaussian 98*, rev. A5; Gaussian, Inc.: Pittsburgh, PA, 1998.

Table 1. Effective Bimolecular Rate Coefficients[a,b] Measured for the Sequential Reactions of $Mg^{+\bullet}$, $(c\text{-}C_5H_5)Mg^+$, and $(c\text{-}C_5H_5)_2Mg^{+\bullet}$ with Hydrogen Cyanide and Cyanoacetylene Proceeding at (294 ± 3) K in a Helium Buffer Gas at a Total Pressure of 0.35 ± 0.01 Torr[c]

ligand[d]	$Mg^{+\bullet}$	$(c\text{-}C_5H_5)Mg^+$	$(c\text{-}C_5H_5)_2Mg^{+\bullet}$
HCN	NR,[e] $<1 \times 10^{-13}$ [3.9×10^{-9}]	$(2.3 \pm 0.7) \times 10^{-9}$ [3.1×10^{-9}]	$\underline{(3.0 \pm 1.0) \times 10^{-9}}$ [2.9×10^{-9}]
2		$(1.2 \pm 0.4) \times 10^{-9}$	$(1.8 \pm 0.6) \times 10^{-9}$
3		$>2.1 \times 10^{-10}$	$>2.0 \times 10^{-10}$
HCCCN	$(1.3 \pm 0.4) \times 10^{-9}$ [4.4×10^{-9}]	$(1.7 \pm 0.5) \times 10^{-9}$ [3.1×10^{-9}]	$\underline{(3.2 \pm 1.0) \times 10^{-9}}$ [2.9×10^{-9}]
2	$(3.1 \pm 1.0) \times 10^{-9}$	$(3.2 \pm 1.0) \times 10^{-9}$	$(2.9 \pm 1.0) \times 10^{-9}$
3	$(1.1 \pm 0.4) \times 10^{-9}$	$(5.8 \pm 1.7) \times 10^{-10}$	$(8.9 \pm 2.7) \times 10^{-10}$
4	$(2.2 \pm 1.1) \times 10^{-9}$	$(6.8 \pm 3.4) \times 10^{-11}$	$(1.2 \pm 0.6) \times 10^{-10}$
5	$(8.3 \pm 4.2) \times 10^{-10}$	$<10^{-12}$	$<10^{-12}$
6	$(1.7 \pm 0.9) \times 10^{-9}$		
7	$(3.7 \pm 1.9) \times 10^{-12}$		
8	$<5 \times 10^{-12}$		

[a] Reaction rate coefficients are given in units of cm^3 $molecule^{-1}$ s^{-1}. Both the rate coefficient and estimated uncertainty are given in parentheses. [b] Collision rate coefficients are given in units of cm^3 $molecule^{-1}$ s^{-1}. Collision rate coefficients are given in square brackets and are calculated using the algorithm of the modified variational transition-state/classical trajectory theory developed by Su and Chesnavich.[24] [c] All the observed reactions, except those underlined, are ligation reactions. The underlined rate coefficients refer to ligand switching reactions. [d] The number of the step in the reaction sequence is given in bold. [e] NR indicates that no reaction was observed.

be denoted as B3LYP/6-31+G(d). In addition, Hartree−Fock and second-order Moller−Plesset calculations were performed at HF/6-31+G(d) and MP2(fc)/6-31+G(d). The optimized geometries at B3LYP/6-31+G(d) and HF/6-31+G(d) were characterized by harmonic frequency calculations, and these established that all the reported structures are at minima. The frequency calculations also yielded both zero-point energies, which are unscaled at B3LYP/6-31+G(d) and scaled by 0.89 at HF/6-31+G(d), and thermal corrections for all the ions.

4. Results and Discussion

Table 1 summarizes the rate coefficients measured for the primary- and higher-order reactions initiated by $Mg^{+\bullet}$, $(c\text{-}C_5H_5)Mg^+$, and $(c\text{-}C_5H_5)_2Mg^{+\bullet}$ in HCN and HC_3N. Overall, the chemistry was dominated by ligation reactions, although an initial ligand-switching reaction was observed with $(c\text{-}C_5H_5)_2Mg^{+\bullet}$. Electron transfer reactions are energetically unfavorable because of the high ionization energies of HCN and HC_3N, IE(HCN) = 13.60 ± 0.01 eV and IE(HC_3N) = 11.62 ± 0.03 eV, compared to IE(Mg) = 7.646 eV.[23] All rate coefficients in Table 1 are *effective bimolecular rate coefficients* measured at 294 ± 3 K and a helium buffer-gas pressure of 0.35 ± 0.01 Torr and are compared with collision rate coefficients computed using the algorithm of the modified variational transition-state/classical trajectory theory developed by Su and Chesnavich[24] with α(HCN) = 2.59 Å^3,[25] μ_D(HCN) = 2.98 D,[26] α(HC_3N) = 5.29 Å^3 (calculated from bond and group polarizabilities)[27] and μ_D(HC_3N) = 3.72 D.[26] The ligation is presumed to occur by termolecular association with the He buffer-gas atoms acting as the stabilizing third body. However, ligation by radiative association, or a contribution to ligation by radiative association, could not be ruled out as the rate coefficients were not measured as a function of the total pressure of helium.

4.1. Reactions with Hydrogen Cyanide.

4.1.a. Reactions with $Mg^{+\bullet}$. No reaction was observed between $Mg^{+\bullet}$ and HCN, $k < 10^{-13}$ cm^3 $molecule^{-1}$ s^{-1},

$$Mg^{+\bullet} + HCN \rightarrow \text{no reaction} \qquad (7)$$

not even the ligation of HCN to $Mg^{+\bullet}$ which is exothermic. We have found that the binding energy at 298 K of hydrogen cyanide to $Mg^{+\bullet}$ at B3LYP/6-31+G(d) is 31.7 kcal mol^{-1}; this result compares favorably with the computed value of 31.9 kcal mol^{-1} reported by Petrie and Dunbar[11a] and a subsequent value of 31.1 kcal mol^{-1} computed by Petrie[11b] at G2(MP2). The rate of the addition reaction 7 is determined by the lifetime of the $[Mg-NCH^{+\bullet}]^*$ intermediate formed initially against dissociation back into $Mg^{+\bullet}$ and HCN; there are two mechanisms by which the intermediate may be stabilized: by collisions with the buffer gas or by emission of radiation. Apparently this lifetime is too short for either mode of stabilization to occur sufficiently rapidly for its observation under our operating conditions within the dynamic range of our rate coefficient measurements. The lifetime can be expected to be short since 31.7 kcal mol^{-1} is a relatively small binding energy and the triatomic HCN can provide only a few degrees of freedom to the $[Mg-NCH^{+\bullet}]^*$ intermediate to distribute the excess energy.[14] The upper limit of 10^{-13} cm^3 $molecule^{-1}$ s^{-1} measured for reaction 7 is consistent with the computed rate coefficient of 1.0×10^{-16} cm^3 $molecule^{-1}$ s^{-1} for radiative association at 100 K.[11] The rate coefficient for radiative association is expected to be even smaller at 300 K.

(19) (a) Hohenburg, P.; Kohn, W. *Phys. Rev. B* **1964**, *136*, 864. (b) Kohn, W.; Sham, L. J. *Phys. Rev. A* **1965**, *140*, 1133. (c) Salahub, D. R.; Zerner, M. C. *The Challenge of d and f Electrons*; American Chemical Society: Washington, DC, 1989. (d) Parr, R. G.; Yang, W. *Density Functional Theory of Atoms and Molecules*. Oxford University Press: Oxford, UK, 1989. (e) Perdew, J. P.; Wang, Y. *Phys. Rev. B* **1992**, *45*, 244. (f) Perdew, J. P.; Chevery, J. A.; Vosko, S. H.; Jackson, K. A.; Pederson, M. R.; Singh, D. J.; Fiolhais, C. *Phys. Rev. B* **1992**, *46*, 6671. (g) Labanowski, J. K.; Andzelm, J. W. *Density Functional Methods in Chemistry*; Springer-Verlag: New York, 1991. (h) Sosa, C.; Lee, C. *J. Chem. Phys*. **1993**, *98*, 8004. (i) Andzelm, J.; Wimmer, E. *J. Chem. Phys*. **1992**, *96*, 1280. (j) Scuseria, G. E. *J. Chem. Phys.* **1992**, *97*, 7528. (k) Becke, A. D. *J. Chem. Phys*. **1992**, *97*, 9173. (l) Becke, A. D. *J. Chem. Phys*. **1992**, *96*, 2155. (m) Gill, P. M. W.; Johnson, B. G.; Pople, J. A.; Frisch, M. J. *Chem. Phys. Lett.* **1992**, *197*, 499. (n) Stephens, P. J.; Devlin, F. J.; Chabalowski, C. F.; Frisch, M. J. *J. Phys. Chem.* **1994**, *98*, 11623. (o) Becke, A. D. Density-Functional Thermochemistry. III. The Role of the Exact Exchange. *J. Chem. Phys*. **1993**, *98*, 5648.
(20) Slater, J. C. *The Self-Consistent Field for Molecules and Solids*; Quantum Theory of Molecules and Solids, Vol. 4; McGraw-Hill: New York. 1974.
(21) Lee, C.; Yang, W.; Parr, R. G. *Phys. Rev. B* **1988**, *37*, 785.
(22) Miehlich, B.; Savin, A.; Stoll, H.; Preuss, H. *Chem. Phys. Lett.* **1989**, *157*, 200.
(23) Lias, S. G.; Bartmess, J. E.; Liebman, J. F.; Holmes, J. L.; Levin, R. D.; Mallard, W. G. Ion Energetics Data. In *NIST Chemistry WebBook;* NIST Standard Reference Database, Number 69; Mallard, W. G., Linstrom, P. J., Eds.; National Institute of Standards and Technology: Gaithersburg MD, February 2000; 20899 (http://webbook.nist.gov).
(24) Su, T.; Chesnavich, J. *J. Chem. Phys.* **1982**, *76*, 5183−5185.
(25) Hirschfelder, J. O.; Curtis, C. F.; Bird, R. B. *Molecular Theory of Gasese and Liquids*; John Wiley & Sons: New York 1954.
(26) Nelson, R. D.; Lide D. R.; Maryott, A. A. NSRDS-NBS 10, 1967.
(27) Lippencott, E. R.; Stutman, J. M. *J. Phys. Chem.* **1964**, *68*, 2926.

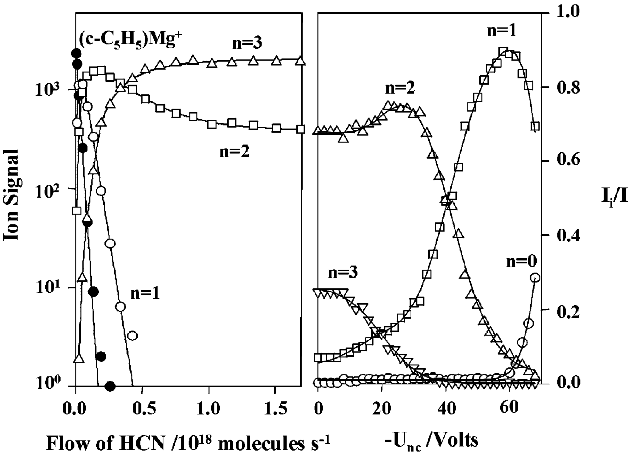

Figure 1. (Left) Experimental data recorded for the sequential addition of hydrogen cyanide to (c-C_5H_5)Mg$(HCN)_n^+$ in a helium buffer gas at 294 ± 3 K and 0.35 ± 0.01 Torr. Rate coefficients derived from the fits are given in Table 1. (Right) Results of *multi*-CID experiments. The fractional abundancies of ion signals for (c-C_5H_5)Mg$(HCN)_n^+$ are plotted against the nose-cone potential, U_{nc}. The flow of hydrogen cyanide is 3.0 × 10^{17} molecules s^{-1}.

4.1.b. Reactions with (c-C_5H_5)Mg^+ and (c-C_5H_5)$_2Mg^{+\bullet}$. The half sandwich, (c-C_5H_5)Mg^+ and the full sandwich, (c-C_5H_5)$_2$-$Mg^{+\bullet}$ both react rapidly with HCN, as can be seen in Figure 1 for the reaction of (c-C_5H_5)Mg^+. The effective bimolecular rate coefficient for the primary addition reaction of the half sandwich is 2.3 × 10^{-9} cm^3 molecule^{-1} s^{-1}, and Table 1 shows that this is equal to the collision rate coefficient, within experimental error. Thus, the (c-C_5H_5) ligand has increased the lifetime of the [(c-C_5H_5)Mg−NCH^+]* intermediate enough to increase the rate of addition by more than a factor of 10^4. We have observed such an enhancement previously for ligation with saturated hydrocarbons, RH, and have attributed the increase in the lifetime of the intermediate complex to the larger number of degrees of freedom available for energy redisposition with (c-C_5H_5)$MgRH^+$ and a higher RH ligand binding energy due to an increased effective charge on Mg.[3] A similar situation should apply here with HCN. The intermediate is expected to be stabilized by collisions with the He buffer-gas atoms. Two more HCN molecules were observed to add to (c-C_5H_5)Mg$(HCN)^+$ as illustrated in reaction 8.

$$(c\text{-}C_5H_5)Mg(HCN)_{n-1}{}^+ + HCN \rightarrow (c\text{-}C_5H_5)Mg(HCN)_n{}^+ \quad (n = 1-3) \quad (8)$$

The second addition also proceeds rapidly, $k = 1.2 \times 10^{-9}$ cm^3 molecule^{-1} s^{-1}, and an equilibrium is established between (c-C_5H_5)Mg$(HCN)_2^+$ and (c-C_5H_5)Mg$(HCN)_3^+$ at high HCN flows (see Figure 1). Because of this, only a lower limit has been quoted for the rate coefficient for the addition of the third HCN molecule. The plot of the ion signal ratio (c-C_5H_5)Mg-$(HCN)_3^+$/(c-C_5H_5)Mg$(HCN)_2^+$ against HCN flow becomes linear at high HCN flows as equilibrium is achieved and provides a standard free-energy change, $\Delta G°$, of −10 kcal mol^{-1}.

CID measurements taken at high flows of HCN show that (c-C_5H_5)Mg$(HCN)_3^+$ loses HCN molecules sequentially with the first HCN loss occurring at very low voltages (see Figure 1).

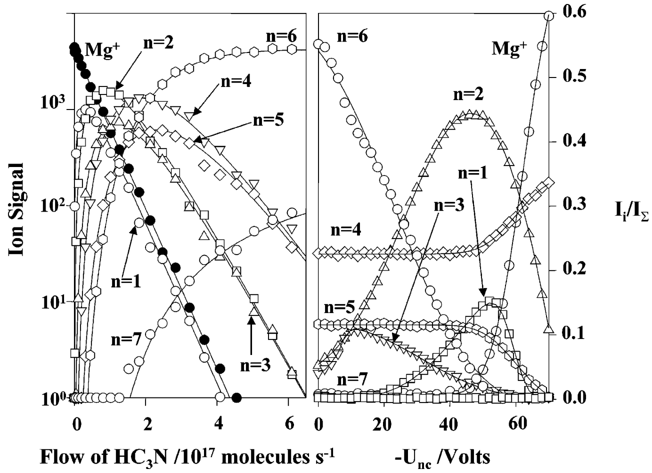

Figure 2. (Left) Experimental data recorded for the sequential addition of cyanoacetylene to $Mg(HC_3N)_n^+$ in a helium buffer gas at 294 ± 3 K and 0.35 ± 0.01 Torr. Rate coefficients derived from the fits are given in Table 1. (Right) Results of *multi*-CID experiments. The fractional abundance of ion signals for $Mg(HC_3N)_n^+$ are plotted against the nose-cone potential, U_{nc}. The flow of cyanoacetylene is 3.6 × 10^{17} molecules s^{-1}.

The reaction of the full sandwich with HCN leads to the switching of HCN with one of the cyclopentadienyl rings to produce, (c-C_5H_5)Mg$(HCN)^+$ according to reaction 9

$$(c\text{-}C_5H_5)_2Mg^{+\bullet} + HCN \rightarrow (c\text{-}C_5H_5)Mg(HCN)^+ + c\text{-}C_5H_5{}^\bullet \quad (9)$$

with a rate coefficient of 3.0 × 10^{-9} cm^3 molecule^{-1} s^{-1}, which is slightly larger than that for the direct addition of HCN to the half sandwich. After the switching reaction, the subsequent chemistry was observed to be identical to that of the half sandwich. The rapid occurrence of reaction 9 at room-temperature implies that D((c-C_5H_5)Mg^+−HCN) > D((c-C_5H_5)Mg^+ − (c-$C_5H_5^\bullet$)).

4.2. Reactions with Cyanoacetylene.

4.2.a. Reactions with $Mg^{+\bullet}$. Unexpectedly and in sharp contrast to HCN, cyanoacetylene was seen to add 7 times in succession to $Mg^{+\bullet}$! Figure 2 shows that these additions proceed sequentially according to reaction 10.

$$Mg(HC_3N)_{n-1}{}^{+\bullet} + HC_3N \rightarrow Mg(HC_3N)_n{}^{+\bullet} \quad (n = 1-7) \quad (10)$$

The much higher rate coefficient for the addition of the first HC_3N, $k = 1.3 \times 10^{-9}$ cm^3 molecule^{-1} s^{-1}, compared to that for HCN addition, $k < 10^{-13}$ cm^3 molecule^{-1} s^{-1}, can be attributed to the higher number of effective degrees of freedom available for energy redisposition in the intermediate complex with HC_3N and a higher binding energy that is expected from the higher polarizability and dipole moment of HC_3N. Petrie and Dunbar report a computed binding energy D($Mg^{+\bullet}$ − NC_3H) = 36.3 kcal mol^{-1} (obtained at a lower level of theory than D($Mg^{+\bullet}$ − NCH) = 31.7 kcal mol^{-1}).[11a,12b] The more recent value computed at G2(MP2) by Petrie is 35.7 kcal mol^{-1}.[11b]

The ion profiles in Figure 2 reveal a very remarkable pattern of reactivity. The second, fourth, and sixth cyanoacetylene adducts are formed quickly and react more slowly than the odd numbered adducts. This is clearly evident in Figure 3 where the alternating patterns in the rate coefficients for addition that

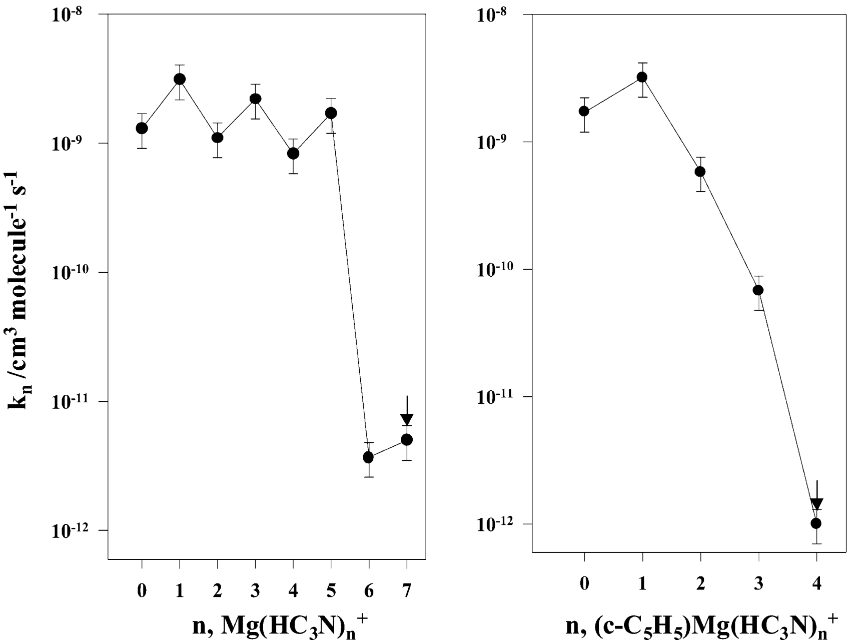

Figure 3. Semilogarithmic plots of the rate coefficient for addition of cyanoacetylene to $Mg^{+\bullet}$ (left) and (c-C_5H_5)Mg^+ (right) as a function of the number of ligands n in the reacting $Mg(HC_3N)_n^{+\bullet}$ or (c-C_5H_5)$Mg(HC_3N)_n^{+\bullet}$ ion. The arrows indicate upper limits.

are extracted from curve fitting the ion profiles in Figure 2 are displayed. Actual values are presented in Table 1. This pattern of reactivity suggests that a special stability is associated with each of the second, fourth, and sixth adducts, perhaps through the formation of cyclic ions due to ligand−ligand interactions mediated by $Mg^{+\bullet}$. The addition of the seventh HC_3N molecule is very slow, $k = 3.7 \times 10^{-12}$ cm^3 molecule^{-1} s^{-1}, which suggests that the seventh HC_3N molecule interacts more weakly, perhaps through electrostatic interaction.

Special stabilities for some $Mg(HC_3N)_n^{+\bullet}$ ions and therefore the occurrence of ligand−ligand interactions are also suggested by the CID results shown in Figure 2. The CID profiles are quite varied in shape and somewhat complicated to interpret. Apparently HC_3N generally is not lost sequentially one at a time; $(HC_3N)_n$ clusters of various sizes appear to be lost instead. The neutral products are, of course, not identified in our experiments nor is the nature of any intracluster chemical bonding, but because of this bonding, the elimination of clusters should be energetically favored over the elimination of individual molecules. Reactions 11a−11g summarize the fragmentation channels that can be discerned from Figure 2.

$$Mg(HC_3N)_6^{+\bullet} \rightarrow Mg(HC_3N)_2^{+\bullet} + [(HC_3N)_4] \quad (11a)$$

$$Mg(HC_3N)_6^{+\bullet} \rightarrow Mg(HC_3N)_3^{+\bullet} + [(HC_3N)_3] \quad (11b)$$

$$Mg(HC_3N)_5^{+\bullet} \rightarrow Mg(HC_3N)_4^{+\bullet} + [HC_3N] \quad (11c)$$

$$Mg(HC_3N)_4^{+\bullet} \rightarrow \textit{does not dissociate} \quad (11d)$$

$$Mg(HC_3N)_3^{+\bullet} \rightarrow Mg(HC_3N)^{+\bullet} + [(HC_3N)_2] \quad (11e)$$

$$Mg(HC_3N)_2^{+\bullet} \rightarrow Mg^{+\bullet} + [(HC_3N)_2] \quad (11f)$$

$$Mg(HC_3N)^{+\bullet} \rightarrow Mg^{+\bullet} + [HC_3N] \quad (11g)$$

As is evident from the CID profiles in Figure 2, *$Mg^{+\bullet}$ coordinated to four cyanoacetylene ligands, $Mg(HC_3N)_4^{+\bullet}$, is unique in that it is very stable*. Another interesting feature to note from the CID profiles is that $Mg(HC_3N)_6^{+\bullet}$ appears to lose neutral cyanoacetylene trimer at a low-energy onset and a tetramer at higher energies. Finally, we cannot rule out some dissociation of $Mg(HC_3N)_3^{+\bullet}$ into $Mg(HC_3N)_2^{+\bullet}$.

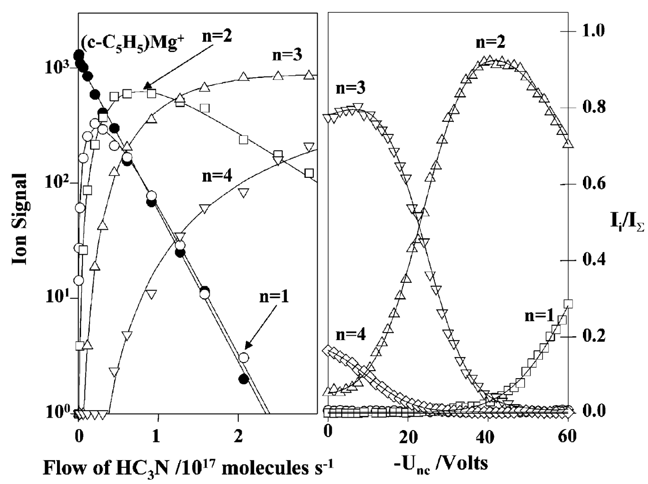

Figure 4. (Left) Experimental data recorded for the sequential addition of cyanoacetylene to (c-C_5H_5)Mg^+ to form (c-C_5H_5)$Mg(HC_3N)_n^+$ in a helium buffer gas at 294 ± 3 K and 0.35 ± 0.01 Torr. Rate coefficients derived from the fits are given in Table 1. (Right) Results of *multi*-CID experiments. The fractional abundance of ion signals for (c-C_5H_5)$Mg(HC_3N)_n^+$ are plotted against the nose-cone potential, U_{nc}. The flow of cyanoacetylene is 2.9 × 10^{17} molecules s^{-1}.

4.2.b. Reactions with (c-C_5H_5)Mg^+. The half-sandwich chemistry with cyanoacetylene is very straightforward in comparison with that of $Mg^{+\bullet}$. Figure 4 shows that, in the HC_3N flow regime investigated, three cyanoacetylene molecules add fairly quickly to the half sandwich according to reaction 12.

$$(c\text{-}C_5H_5)Mg(HC_3N)_{n-1}^{+} + HC_3N \rightarrow (c\text{-}C_5H_5)Mg(HC_3N)_n^{+} \quad (n = 1-3) \quad (12)$$

A fourth molecule of HC_3N is seen to add more slowly, perhaps by electrostatic interaction rather than direct ccordination to the magnesium. A semilogarithmic plot of rate coefficient versus the number of ligands, Figure 3, does not show the alternation in the rate coefficient that was seen with $Mg^{+\bullet}$ and so is not suggestive of ligand−ligand interactions. The CID results in Figure 4 show that the successively added HC_3N molecules are removed one at a time as the nose cone voltage is increased, further suggesting that no ligand/ligand interactions had occurred upon formation of the adduct ions by reaction 12.

4.2.c. Reactions with (c-C_5H_5)$_2$$Mg^{+\bullet}$. In the full sandwich chemistry, as was the case with HCN, the first step is the rapid displacement of one c-C_5H_5 ring by cyanoacetylene, $k = 3.2 \times 10^{-9}$ cm^3 molecule^{-1} s^{-1}, according to reaction 13.

$$(c\text{-}C_5H_5)_2Mg^{+\bullet} + HC_3N \rightarrow (c\text{-}C_5H_5)Mg(HC_3N)^+ + c\text{-}C_5H_5^{\bullet} \quad (13)$$

After the ligand switching, the observed chemistry behaves in a manner analogous to that initiated by the half sandwich by adding four cyanoacetylene molecules that are sequentially removed in the CID experiment. The rapid occurrence of reaction 13 suggests that D((c-C_5H_5)Mg^+ − HC_3N) > D((c-C_5H_5)Mg^+ − (c-$C_5H_5^{\bullet}$)).

5. Structures and Bonding of $Mg(HC_3N)_n^{+\bullet}$.

The unusual periodicity in the rate coefficients for HC_3N ligation and the striking CID profiles seen for the ligated $Mg(HC_3N)_n^{+\bullet}$ ions prompted a theoretical investigation to probe various structures that might be invoked to account for these experimental results.

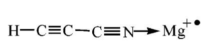

1, C$_{\infty h}$

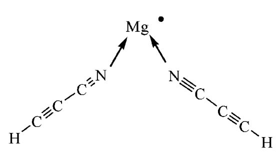

2, C$_{2v}$

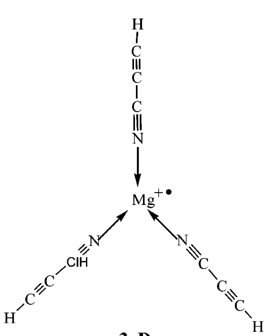

3, D$_{3h}$

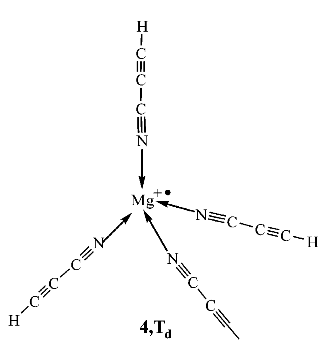

4, T$_d$

Three critical points were found for the first addition of cyanoacetylene to $Mg^{+\bullet}$. In the lowest-energy structure $Mg^{+\bullet}$ binds to the nitrogen atom, forming a linear complex, (structure **1**) that has a binding energy of 36.8 kcal mol^{-1}. The unpaired electron is in the σ-system and is localized on the Mg. The geometry of the ligand changes slightly on complexation, with the largest change being a decrease in the formally single NC−C_2H bond, from 1.373 to 1.360 Å. Two other minima were located on the $Mg(HC_3N)^{+\bullet}$ potential energy surface. One, a π-complex in which the $Mg^{+\bullet}$ is attached to the C−C triple bond, lies 30.6 kcal mol^{-1} above **1** and has a dissociation energy of 6.2 kcal mol^{-1}. The third structure is a high-energy isomer in which the $Mg^{+\bullet}$ is inserted into the C−H bond; this structure lies 39.4 kcal mol^{-1} *above* the reactants, $Mg^{+\bullet}$ plus HC_3N. On the basis of these calculations we conclude that the monoadduct has structure **1**.

Table 2. Electronic Energies (in hartrees), Zero-Point Vibrational Energies and Relative Energies (both in kcal mol^{-1})

ions	B3LYP/6-31+G(d)	ZPE	energy relative to $Mg^{+\bullet}$ + 4 HC_3N
$Mg^{+\bullet}$	−199.79555	−	−
1	−369.43743	18.2	−36.8
2	−539.06292	36.4	−63.3
3	−708.69074	53.7	−92.1
4	−878.28941	70.4	−101.8
5	−539.05335	38.1	−55.6
6	−539.04975	37.6	−53.8
7	−539.04680	37.0	−52.5
8	−708.71603	56.7	−105.0
9	−708.70806	56.3	−100.4
10	−708.68048	56.1	−83.6
11	−878.40404	79.7	−165.8
12	−878.44961	81.1	−193.1
	Neutral Molecules		
Mg	−200.07958	−	
HC_3N	−169.58121	16.9	
	1,2,5,6-Tetracyanocyclooctatetrene		
	−678.55714	79.3	
	2,4,6,8-Tetracyanosemibullvalene		
	−678.55877	80.0	

Next we examined adducts $Mg(HC_3N)_n^{+\bullet}$ with $n = 2$, 3, and 4, each time attaching the Mg directly to the nitrogen of the cyanoacetylene molecules, as in structure **1**. The di-adduct, **2**, is planar with an NMgN angle of 97.8°. Similar ligand−ligand angles were previously found for $Mg^{+\bullet}$/ammonia and $Mg^{+\bullet}$/water complexes.[1,28−32] Another notable feature of structure **2** is that the two ligands are not attached as symmetrically to the Mg as in **1**. The MgNC angles are 164°, with the two ligands bent away from each other. All the other angles in the ligand remain at 180°.

The third adduct, **3**, is trigonal (D_{3h} symmetry) and the fourth, **4**, is tetrahedral (T_d symmetry). In each of these complexes the ligand retains perfect linearity. The calculated binding energies of structures **1**−**4** are given in Table 2. Addition of the first ligand is exothermic by 36.8 kcal mol^{-1}, the second by 26.5 kcal mol^{-1}, and the third by a further 28.8 kcal mol^{-1}. Finally, addition of the fourth ligand to $Mg(HC_3N)_3^{+\bullet}$ is exothermic by only 9.7 kcal mol^{-1}. The slightly higher exothermicity of the third addition relative to that of the second one is puzzling, and these data provide no hint of unusual stability for the fourth adduct.

In complexes containing more than one ligand the CID results indicate that two ligands react. We examined the potential energy surface for $Mg(HC_3N)_2^{+\bullet}$ and found 11 structures at minima. Of these, **2** was found to be the lowest-energy structure, but three other structures, ions **5**, **6**, and **7**, were calculated to

(28) Milburn, R. K.; Bohme, D. K.; Hopkinson, A. C. *J. Mol. Struct*. **2001**, *540*, 5.
(29) Shoeib, T.; Milburn, R. K.; Koyanagi, G. I.; Lavrov, V. V.; Bohme, D. K.; Siu, K. W. M.; Hopkinson, A. C. *Int. J. Mass Spectrom* **2000**, *201*, 87.
(30) Bauschlicher Jr., C. W.; Sodupe, M.; Partridge, H. *J. Chem. Phys.* **1992**, *96*, 4453.
(31) Bauschlicher, C. W., Jr.; Partridge, H. *Chem Phys. Lett.* **1991**, *95*, 3946.
(32) Bauschlicher, C. W. Jr.; Partridge, H. *J. Chem. Phys.* **1991**, *95*, 9694.

be within 11 kcal mol^{-1} of **2** at B3LYP/6-31+G(d). All the additional structures are planar and have the terminal carbon atoms of the cyanoacetylene units linked. Ions **5** and **7** are 7.7 and 10.8 kcal mol^{-1} respectively above **2** in energy and are structurally similar, with a long bond between the central carbon atoms of each cyanoacetylene unit (1.596 Å in **5** and 1.571 Å in **7**), essentially forming distorted cyclobutadienes. Each has nine π-electrons and the major structural difference is that attachment to $Mg^{+\bullet}$ is through both nitrogens in **5** and only through one in **7**. Ion **6** has a different electronic structure with only eight π-electrons and the unpaired electron remaining on the magnesium in the σ-system.

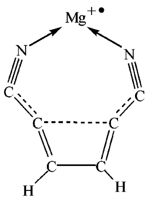
5, C_{2v}

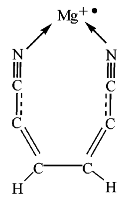
6, C_{2v}

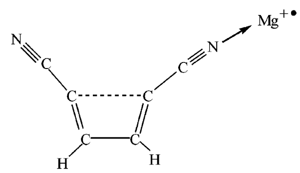
7, C_s

Four structures on the $Mg(HC_3N)_3^{+\bullet}$ potential energy surface were optimized. Each of these is formed by direct addition of a cyanoacetylene molecule through nitrogen to the magnesium atom of the four lowest-energy $Mg(HC_3N)_2^{+\bullet}$ complexes. In this process ion **2** produces **3**, ion **5** produces **8**, ion **6** produces **9**, and ion **7** produces **10** with exothermicities (at 0 K) of 28.8, 49.4, 46.6, and 31.1 kcal^{-1} respectively. Here, on the tri-adduct potential energy surface, unlike on the di-adduct surface, two of the cyclic structures, ions **8** and **9**, have the lowest energies and these are significantly better than that of the product of direct addition of three ligands, ion **3**. The energy of isomer **10** is significantly higher than those of the other three $Mg(HC_3N)_3^{+\bullet}$ isomers and was not considered further. Direct addition of a fourth cyanoacetylene to both **8** and **9** led to only slightly exothermic reactions, as was the case for the fourth addition to **3**.

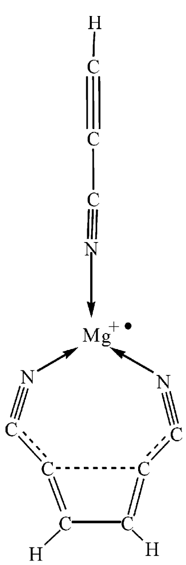
8, C_{2v}

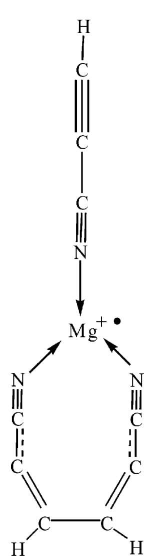
9, C_{2v}

However, in one attempted optimization a structurally quite different complex, 1,2,5,6-tetracyanocyclooctatraene in the boat conformation and coordinated to the $Mg^{+\bullet}$ through all four cyano groups was produced. Formation of this ion (structure **11**) from the lowest-energy isomer on the tri-adduct surface, ion **8**, is exothermic by 60.8 kcal mol^{-1}, in keeping with the unusual stability of the fourth adduct.

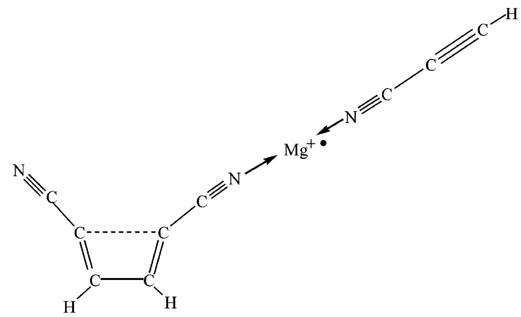
10, C_S

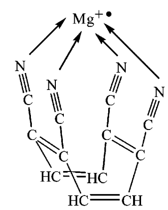
11, C_{2v}

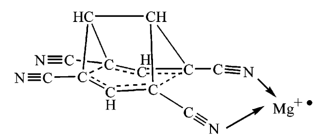
12, C_s

Semibullvalene is an isomer of cyclooctatetraene, and both molecules ionize to produce the *same* radical cation, $C_8H_8^{+\bullet}$.[33,34] CIDNP experiments and computational studies have established that this ion is the nonclassical bicycle[3.3.0]octa-2,6-diene-4,8-diyl radical cation.[35−39]

$Mg(HC_3N)_4^{+\bullet}$ is also a radical cation, albeit with an additional Mg atom, and it therefore seemed possible that this very stable ion is a $Mg^{+\bullet}$/tetracyanocyclosemibullvalene complex. The parent semibullvalene molecule has a classical structure with one cyclopropane ring and two double bonds. However, it undergoes a degenerate Cope-type rearrangement involving a 6π-electron delocalized transition state similar to that shown on structure **12**, that is stabilized by being bishomoaromatic.[40,41] The barrier to this rearrangement is low (experimentally, $\Delta G^{\ddagger}$ is around 6 kcal mol^{-1}). Electron-withdrawing substituents in the 2, 4, 6, and 8 positions are expected to stabilize the symmetrical transition state relative to the classical semibullvalene structure, and previous calculations predicted that the symmetrical nonclassical 2,4,6,8-tetracyanosemibullvalene should be at a minimum.[42,43] We optimized 17 isomers of tetracyanosemibullvalene (first at HF/3-21G and then at B3LYP/6-31+G(d)) and found only two isomers that have the nonclassical structure. One has cyano groups at the 2, 4, 5, and 6

(33) Dai, S.; Wang, J. T.; Williams, F. *J. Am. Chem. Soc*. **1990**, *112*, 2837.
(34) Dai, S.; Wang, J. T.; Williams, F. *J. Am. Chem. Soc*. **1990**, *112*, 2835.
(35) Roth, H. D.; Lakkaraju, P. S. *J. Phys. Chem.* **1993**, *97*, 13403.
(36) Williams, F. *J. Phys. Chem.* **1994**, *98*, 8258.
(37) Williams, F. *J. Chem. Soc., Faraday Soc.* **1994**, *90*, 1681.
(38) Bally, T.; Truttmann, L.; Dai, S.; Williams, F. *J. Am. Chem. Soc*. **1995**, *117*, 7916.
(39) Bally, T.; Truttmann, L.; Dai, S.; Williams, F. *J. Mol. Struct. (THEOCHEM)* **1997**, *398*, 255.
(40) Cheng, A. K.; Anet, F. A. L.; Mioduski, J.; Meinwald, J. *J. Am. Chem. Soc*. **1974**, *96*, 2887.
(41) Moskau, D.; Aydin, R.; Leber, W.; Gunther, H.; Quest, H.; Martin, H. D.; Hassenruck, K.; Miller, L. S.; Grohmann, K. *Chem. Ber.* **1989**, *122*, 925.
(42) Hoffmann, R.; Stohrer, W.-D. *J. Am. Chem. Soc*. **1971**, *93*, 6941.
(43) Dewar, M. J.; Lo, D. J. *J. Am. Chem. Soc*. **1971**, *93*, 7201.

Scheme 1

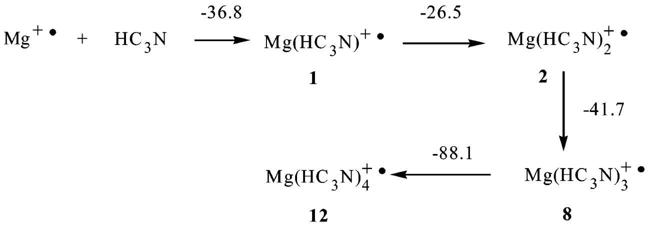

positions and the other at the 2, 4, 6, and 8 positions. The latter isomer had one of the lowest energies, with only two structures being slightly lower (the 1,3,6,7-substituted isomer was the best, 0.7 kcal mol^{-1} lower than the 2,4,6,8-substituted isomer).

Our interest was primarily in the $Mg^{+\bullet}$/tetracyanosemibullvalene complexes. We calculated structures for most of the tetracyanosemibullvalenes at HF/3-21G and found that complexes in which *two* cyano groups are located at the 2 and 4 positions have much higher binding energies (by ~30 kcal mol^{-1}) than those of all other complexes. Optimization of ion **12** at B3LYP/6-31+G(d) gave a structure in which the 6π-electron delocalization is retained. This ion was found to be 27.3 kcal mol^{-1} lower in energy than the four-coordinate $Mg^{+\bullet}$/1,2,5,6-tetracyanocyclooctatrene complex, ion **11**. At B3LYP/6-31+G(d) formation of **12** from **8**, the lowest-energy isomer on the tri-adduct surface, is calculated to be exothermic by 88.1 kcal mol^{-1}, and the binding energy of $Mg^{+\bullet}$ to 2,4,6,8-semibullvalene is 58.7 kcal mol^{-1}.

Assuming that the lowest-energy isomer of each adduct is formed, then the $\Delta H°$ at 0 K (in kcal mol^{-1}) values for each step are as given in Scheme 1.

The kinetics of the sequential addition of HC_3N to $Mg^{+\bullet}$ that was observed experimentally (see Figure 3 (left)) should follow the thermodynamics indicated in Scheme 1 if the stability of the magnesium ion cluster that is formed is the deciding factor in determining the magnitude of the rate coefficient for addition. However, the relatively slow addition of the third HC_3N compared to the second addition is at odds with the larger calculated binding energy of the third ligand (ignoring rearrangement) and the calculated existence of significantly stabilized rearrangement clusters involving three HC_3N ligands (structures **8** and **9**). If the structure of the reacting cluster ion also is important, the rearrangement to stable ring structures promoted by intramolecular ligand−ligand interactions also could account for the relatively lower reactivities of $Mg(HC_3N)_2^{+\bullet}$ and $Mg(HC_3N)_4^{+\bullet}$ with another HC_3N molecule and so the observed alternating pattern in the chemical reactivity of $Mg^{+\bullet}$ with cyanoacetylene.

6. Implications for the Chemistry of the Atmosphere of Titan and for Circumstellar Chemistry

Our laboratory observation of the rapid sequential addition of up to six molecules of cyanoacetylene to $Mg^{+\bullet}$ under He collision-dominated conditions suggests the occurrence of the formation of cyanoacetylene clusters of $Mg^{+\bullet}$ by sequential association in any environment containing cyanoacetylene and magnesium in ionized form. Sequential association may proceed either in termolecular fashion at higher pressures through stabilization of the intermediate complex by collisions with a third molecule, M, or in a bimolecular fashion at low pressures by stabilization through the emission of radiation, or by a

Scheme 2

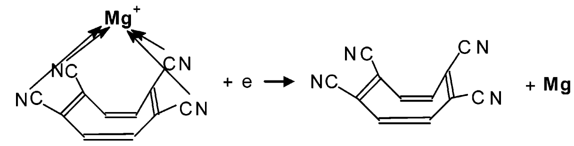

cyclooctatetraene

combination of both in regions of intermediate pressures. Cyanoacetylene cluster formation by sequential radiative association is indicated by reaction 14a, in analogy with radiative association of the first cyanoacetylene molecule, reaction 3, while sequential collisional association is indicated by reaction 14b.

$$Mg(HC_3N)_{n-1}{}^{+\bullet} + HC_3N \rightarrow Mg(HC_3N)_n{}^{+\bullet} + h\nu \quad (14a)$$

$$Mg(HC_3N)_{n-1}{}^{+\bullet} + HC_3N + M \rightarrow Mg(HC_3N)_n{}^{+\bullet} + M \quad (14b)$$

The recombination of $Mg(HC_3N)_n{}^{+\bullet}$ with electrons, according to reaction 15, can provide a route to the formation of cyano derivatives of large unsaturated hydrocarbons in environments containing $Mg^{+\bullet}$, cyanoacetylene, and electrons.

$$Mg(HC_3N)_n{}^{+\bullet} + e \rightarrow Mg + [(HC_3N)_n] \quad (15)$$

Of course, sequential ligation must compete with electron−ion recombination, and this competition is governed by the relative abundance of electrons and cyanoacetylene in the environment in question. Also, the neutral products of reaction 15 are still very much a matter of speculation.

Our computations and CID experiments suggest that the $Mg(HC_3N)_{2,3}{}^{+\bullet}$ adducts formed in reaction 14 may neutralize by recombination with electrons to produce cyclobutadiene derivatives with CN substituents. Furthermore, the computations indicate that the four cyanoacetylene molecules in the stable structure found for $Mg(HC_3N)_4{}^{+\bullet}$ are attached to magnesium either in the boat form of 1,2,5,6-tetracyano-1,3,5,7-cyclooctatetraene which contains the cyclic eight-carbon backbone of the well-known cyclooctatetraene molecule, or as 2,4,6,8-tetracyanosemibullvalene. Thus, electron−ion recombination of the extraordinarily stable $Mg(HC_3N)_4{}^{+\bullet}$ cluster ion according to reaction 15 should produce either the boat (tub) form of 1,2,5,6-tetracyano-1,3,5,7-cyclooctatetraene as shown in Scheme 2, or 2,4,6,8-tetracyanosemibullvalene. Our DFT calculations indicate that the recombination to form the semibullvalene is exothermic by 58.7 kcal mol^{-1} at 0 K and that to form the cyclooctatetraene is exothermic by 31.8 kcal mol^{-1} at 0 K. The exothermicity of the latter recombination is not sufficient to allow for the isomerization of the boat to the chair form. The chair form is computed to be 51.7 kcal mol^{-1} higher in energy at 0 K (previous calculations for the underivatized cyclooctatetraene molecule show a similar energy difference of between 54.8 and 58.0 kcal mol^{-1}, depending on the level of theory[46]). Furthermore, the chemistry identified here suggests analogous synthetic opportunities with the higher-order cyanopolyacetylenes.

(44) Szabo, K. J.; Cremer, D. Quoted by Childs, R. F.; Cremer, D.; Elia, D. In *Chemistry of the Cyclopropyl Group*; Rappoport, Z., Ed.; John Wiley & Sons: Chichester, 1995; Vol. 2, p 455.
(45) Fukasaku, S.; Hirahara, Y.; Masuda, A.; Kawaguchi, K.; Ishikawa, S.; Kaifu, N.; Irvine, W. M. *Astrophys. J.* **1994**, *437*, 410.
(46) Andrés, J. L.; Castarño, O.; Morreale, A.; Palmeiro, R.; Gomperts, R. *J. Chem. Phys.* **1998**, *108*, 203.

$Mg^{+\bullet}$ arises by meteoritic ablation mainly at altitudes between 600 and 800 km under the conditions expected in the atmosphere of Titan where cyanoacetylene is taken to be the third most abundant nitrogen-containing compound. Petrie already has suggested that ligand-switching involving less strongly bonded $Mg^{+\bullet}$ adduct ions will ultimately establish HC_3N adducts as HC_3N has the highest $Mg^{+\bullet}$ affinity of molecules of any significance at these altitudes.[13] Also, modeling predicts free electron abundances at these altitudes many orders of magnitude below the abundance of cyanoacetylene. This means that sequential addition of cyanoacetylene becomes feasible and complex organomagnesium ions of the type observed in our experiments may be formed in Titan's atmosphere. Electron−ion recombination of these ions may then produce organomagnesium neutrals or organic cyanides including even tetracyanosemibullvalene, tetracyanocyclooctatetraene, or other cyclic molecules derivatized with cyanocontaining substituents in the regeneration of Mg.

The opposite is expected to be true in circumstellar environments in which the electron abundance far exceeds that of cyanoacetylene. Rate coefficients for the radiative association of cyanopolyacetylenes with $Mg^{+\bullet}$ have been shown by calculation to be sufficiently high to make these molecules effective scavengers for $Mg^{+\bullet}$ in cold dark clouds in their early chemistry (Dunbar and Petrie, 2002). For example, they lead to lifetimes from 1.8×10^5 years for HC_3N to as little as 450 years for HC_7N in TMC-1.[12b] However, the higher-order radiative cyanoacetylene association, reaction 14a, while expected to become more efficient with increasing number of molecules, must compete with electron−ion recombination which acts to revert the chemistry by reaction 2 back to reactants or possibly also to cyanoacetylene dissociation. In fact, based on the modeled abundancies of HC_3N and free electrons in these environments, any $Mg(HC_3N)^{+\bullet}$ adducts will be lost primarily by dissociative recombination with electrons such as reaction 4 rather than by subsequent radiative association with HC_3N, reaction 14a.

Conclusions

The measured kinetics of the gas-phase ligation of $Mg^{+\bullet}$ and $(c\text{-}C_5H_5)Mg^+$ with hydrogen cyanide and cyanoacetylene at room temperature in helium at 0.35 Torr is consistent with termolecular collision-stabilized association. The tri-atomic hydrogen cyanide molecule does not ligate to magnesium radical cations under these conditions, while the five-atom cyanoacetylene molecule ligates sequentially up to seven times in the reaction time of ca. 5 ms. A remarkable alternating pattern is exhibited in the rate of ligation of cyanoacetylene to atomic magnesium radical cations while multiple-collision induced dissociation experiments reveal an extraordinary stability for the $Mg(HC_3N)_4^{+\bullet}$ cluster ion. The alternating pattern in the chemical reactivity of $Mg^{+\bullet}$ with cyanoacetylene disappears in the presence of a cyclopentadienyl ligand, but sequential cyanoacetylene addition still occurs. $(c\text{-}C_5H_5)_2Mg^{+\bullet}$ reacts simply and rapidly with cyanoacetylene by ligand switching to establish $(c\text{-}C_5H_5)Mg(HC_3N)^+$, just as with hydrogen cyanide to establish $(c\text{-}C_5H_5)Mg(HCN)^+$.

DFT molecular orbital calculations indicate that the path to formation of $Mg(HC_3N)_4^{+\bullet}$ involves ligand−ligand interactions leading to two cyclic $(HC_3N)_2$ ligands which then interact to lead to the formation of 2,4,6,8-tetracyanosemibullvalene-Mg^+ or 1,2,5,6-tetracyano-1,3,5,7-cyclooctatetraene-Mg^+ cations. The formation of stable ring structures promoted by intramolecular ligand−ligand interactions in $Mg(HC_3N)_2^{+\bullet}$ and $Mg(HC_3N)_4^{+\bullet}$ also could account for the relatively lower reactivities of these two cluster ions with HC_3N and thus the observed alternating pattern in the chemical reactivity of $Mg^{+\bullet}$ with cyanoacetylene.

Finally, we propose that formation of complex organomagnesium ions of the type observed in our experiments with HC_3N should occur in the upper atmosphere of Titan where subsequent electron−ion recombination might lead to the formation of cyano derivatives of large unsaturated hydrocarbons, possibly the boat form of 1,2,5,6-tetracyano-1,3,5,7-cyclooctatetraene or even 2,4,6,8-tetracyanobullvalene. In contrast, circumstellar environments containing $Mg^{+\bullet}$ and cyanoacetylenes are less likely to give rise to such chemistry because of the much higher relative content of free electrons.

Acknowledgment. Continued financial support from the Natural Sciences and Engineering Research Council of Canada is greatly appreciated. As holder of a Canada Research Chair in Physical Chemistry, D.K.B. thanks the Canada Research Chair Program for its contributions to this research. We also thank Joey Cheng for her contributions to the calculations.

Supporting Information Available: Detailed structural information derived from the molecular orbital calculations; the complete ref 18. This material is available free of charge via the Internet at http://pubs.acs.org.

JA053302F